

# Scanning Electrochemical Microscopy, 52. Bipolar Conductance Technique at Ultramicroelectrodes for Resistance Measurements

Robert J. LeSuer, Fu-Ren F. Fan, and Allen J. Bard\*

Department of Chemistry and Biochemistry, The University of Texas at Austin, Austin, Texas 78712

The bipolar conductance, BICON, technique for the measurement of solution resistance, based on the application of microsecond current pulses, as originally described by Enke and co-workers for measurements with conventional electrodes, was extended for use with ultramicroelectrodes, with a focus on its application in scanning electrochemical microscopy (SECM). When the plateau time used to make the measurement lies within the BICON conditions, the solution conductance can be obtained directly from the output without the need for calibration curves. However, decreasing the size of the ultramicroelectrode decreases the range of values that satisfy these conditions, and one must resort to calibration curves to obtain solution conductance from the measured current, which was nevertheless found to be proportional to electrolyte concentration with electrodes as small as 5  $\mu\text{m}$  in diameter. BICON/SECM approach curves over insulating substrates followed SECM negative feedback theory and approach curves in the presence of low (micromolar) or no added electrolyte are possible once the background conductivity is taken into account. Approach curves to a conducting substrate at open circuit potential are influenced by the solution time constant (solution resistance at the electrode tip  $\times$  electrode double layer capacitance), which is a function of the tip/substrate distance, as well as the substrate size.

Over 30 years ago, Johnson and Enke described a novel technique for the facile measurement of solution conductance using a bipolar DC pulse.<sup>1</sup> This bipolar conductance (BICON) technique utilizes a pair of square-wave potential pulses with equal durations and equal but opposite polarities to obtain a single point analysis of the current that yields the solution conductance at the end of the pulse sequence. When the duration of the pulse is chosen so that it satisfies the BICON conditions, as discussed below, current due to charging of the electrode double layer is corrected for, and the solution conductance can be obtained directly from the output.

The BICON technique has found many uses. Since it has been shown that the slope of the conductance versus concentration curve changes at the critical micelle concentration (CMC), Nieman et al. coupled BICON to an exponential dilutor to rapidly (10 min)

determine surfactant CMCs.<sup>2</sup> Soper et al. incorporated two 127- $\mu\text{m}$  Pt disks into poly(methyl methacrylate) microfluidic devices and used BICON as a conductometric detector for monitoring the separation of amino acids, peptides, and proteins.<sup>3</sup> Sandifer and Gross attempted to utilize the BICON technique with calcium ion-selective electrodes,<sup>4</sup> but observed no conductance changes when measuring  $\text{Ca}^{2+}$  in the presence of a large excess of KCl. The technique has undergone several modifications since its conception, one<sup>5</sup> to accommodate advances in chip technology and another by Nieman et al.,<sup>6</sup> who added constant current pulses and resistor banks for a wider dynamic range. We have selected this technique when faced with the necessity of measuring conductance changes during irradiation of photoresists in 18 M $\Omega$ -cm water, a process of importance to immersion lithography.<sup>7</sup>

Conductance measurements at solid/liquid interfaces with scanning probes are of interest, especially under conditions in which the ionic species under investigation are not electroactive. Thus, several research groups have implemented conductance measurements using SECM or related techniques. A scanning conductance microscope was described in 1989 by Hansma and co-workers, who used an electrolyte-filled micropipet to measure local ion currents above a surface.<sup>8</sup> In SECM, conductance measurements share an advantage with potentiometric modes, namely, the ability to probe an interface without significantly perturbing the system under investigation. Unlike potentiometric modes, conductometric measurements follow SECM approach feedback theory when the microelectrode tip approaches an insulating substrate.<sup>9</sup> This allows for an accurate measurement of the tip–substrate distance, an essential parameter for obtaining quantitative information. Several others have explored conductance measurements in the SECM geometry. Horrocks et al.<sup>9</sup> used AC

- (2) (a) Baxter-Hammond, J.; Powley, C. R.; Cook, K. D.; Nieman, T. A. *J. Colloid Interface Sci.* **1980**, *76*, 434. (b) Taylor, D. W.; Nieman, T. A. *Anal. Chem.* **1984**, *56*, 593.
- (3) Galloway, M.; Stryjewski, W.; Henry, A.; Ford, S. M.; Llopis, S.; McCarley, R. L.; Soper, S. A. *Anal. Chem.* **2002**, *74*, 2407.
- (4) Sandifer, J. R.; Gross, S. *Anal. Chim. Acta* **1987**, *192*, 237–242.
- (5) Caserta, K. J.; Holler, F. J.; Crouch, S. R.; Enke, C. G. *Anal. Chem.* **1978**, *50*, 1534.
- (6) Calhoun, R. K.; Holler, F. J.; Geiger, R. F.; Nieman, T. A.; Caserta, K. J. *Anal. Chim. Acta* **1991**, *252*, 29.
- (7) LeSuer, R. J.; Fan, F.-R. F.; Bard, A. J.; Taylor, J. C.; Tsiartas, P.; Willson, G.; Conley, W. E.; Feit, G.; Kunz, R. R. *Proc. SPIE-Int. Soc. Opt. Eng.* **2004**, *5376*, 115.
- (8) Hansma, P. K.; Drake, B.; Marti, O.; Gould, S. A.; Prater, C. B. *Science* **1989**, *243*, 641.
- (9) Horrocks, B. R.; Schmidtke, D.; Heller, A.; Bard, A. J. *Anal. Chem.* **1993**, *65*, 3605.

\* To whom correspondence should be addressed. E-mail: ajbard@mail.utexas.edu.

(1) Johnson, D. E.; Enke, C. G. *Anal. Chem.* **1970**, *42*, 329.

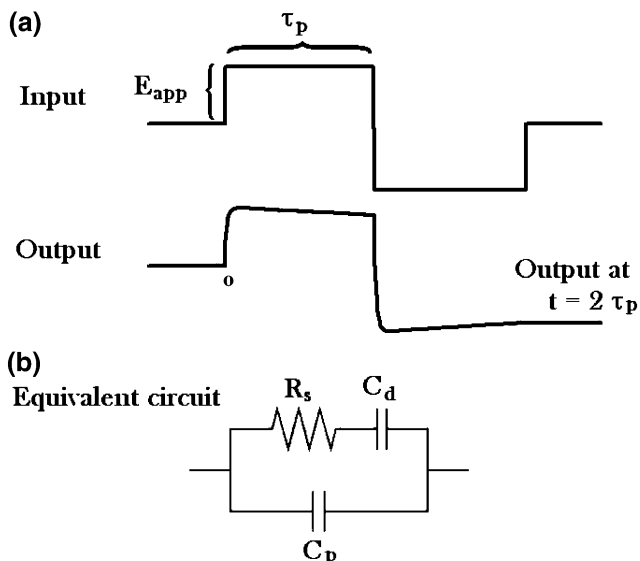


**Figure 1.** Schematic of timing sequence (above) and equivalent circuit (below) used to analyze the electrochemical cell.

conductance measurements at a potentiometric tip to measure tip/substrate distances. Alpuche-Aviles et al.<sup>10</sup> used a similar technique to perform generation/collection experiments at constant tip/substrate separations. Schuhmann et al. used AC conductometric SECM to investigate microcavities in lacquered tinplates, which are thought to be precursor sites for localized corrosion.<sup>11</sup>

In this paper, we briefly review the theory of BICON measurements and describe its application to ultramicroelectrodes. We then analyze the behavior of BICON/SECM approach curves with insulating and conducting substrates and discuss the situations in which BICON/SECM follows amperometric feedback theory.

## THEORY

BICON employs two consecutive pulses with equal durations (plateau times,  $\tau_p$ ) and equal but opposite amplitudes,  $E_{app}$ . A timing schematic is shown in Figure 1a. The equivalent circuit used in the analysis of the electrochemical cell is shown in Figure 1b, where  $R_s$  is the solution resistance,  $C_d$  is the double layer capacitance of the microelectrode, and  $C_p$  is stray capacitance which arises from the instrumental design. Assuming the plateau time,  $\tau_p$ , is at least  $5RC_p$  (where  $R$  is the output impedance of the data acquisition board), the parallel capacitance can be ignored in the circuit analysis. The problem is now simplified to the charging and discharging of a series RC circuit. During the first step, when the time,  $t$ , is less than  $\tau_p$ , with the potential applied to the cell,  $E_{app}$ , the current for the first half of a BICON pulse will be given by<sup>12</sup>

$$i(t)_{t < \tau_p} = \frac{E_{app}}{R_s} (e^{-t/R_s C_d}) \quad (1)$$

Analysis of the second step,  $t > \tau_p$ , follows analogously with an initial condition for the charge on the capacitor evaluated at  $t$

$= \tau_p$ . The BICON pulse is typically symmetric, with a voltage applied in the second step of  $-E_{app}$ . The current observed during the second step of a BICON pulse is then

$$i(t)_{t > \tau_p} = \frac{E_{app}}{R_s} e^{-t/R_s C_d} (1 - 2e^{\tau_p/R_s C_d}) \quad (2)$$

When the ratio of the step time to the cell time constant ( $r_{solution} = \tau_p/R_s C_d$ ) is small, the current at  $t = 2\tau_p$  approaches  $E_{app}/R_s$ , thus allowing the solution resistance to be determined by measurement of the current at the end of a BICON pulse. The difference between the actual and measured resistance depends on  $r_{solution}$

$$\text{error (\%)} = 100e^{-2r_{solution}} (-1 + 2e^{r_{solution}}) \quad (3)$$

For  $r_{solution} = 0.1$ , the actual solution resistance will be 99.1% of the resistance calculated at the end of the BICON pulse from  $E_{app}/R_s$ .

The output observed when a BICON pulse is applied to a microelectrode is also complicated by the finite response time of the amplification circuitry, which must be taken into consideration to obtain a satisfactory simulation of the experimental results. The response time is approximated by multiplying each step of the BICON pulse by an exponential factor with a rise time of  $R_f C_f$ , where  $R_f$  is the input resistance and  $C_f$  is the capacitance of the feedback circuitry. The response from a BICON pulse is now described by

$$i(t) = \begin{cases} \frac{E_{app}}{R_s} e^{-t/R_s C_d} (1 - e^{-t/R_f C_f}) & 0 < t < \tau_p \\ \frac{E_{app}}{R_s} e^{-t/R_s C_d} (1 - e^{-(t-\tau_p)/R_f C_f}) (1 - 2e^{\tau_p/R_s C_d}) & \tau_p < t < 2\tau_p \end{cases} \quad (4)$$

Error in the resistance measurement at  $t = 2\tau_p$  is dependent on the ratio of the plateau time to the feedback time constant, ( $r_{feedback} = \tau_p/R_f C_f$ ) as well as  $r_{solution}$ .

$$\text{error (\%)} = 100e^{-(r_{feedback} + 2r_{solution})} (-1 + e^{r_{feedback}}) (-1 + 2e^{r_{solution}}) \quad (5)$$

For  $r_{solution} = 0.1$  and  $r_{feedback} = 4$ , the actual solution resistance will be 97.3% of the value calculated using the current:  $R_{apparent} = E_{app}/i(2\tau_p)$ .

Ideally, a plateau time can be chosen that is larger than  $R_f C_f$  but significantly smaller than  $R_s C_d$ , such that  $R_f C_f \ll \tau_p \ll R_s C_d$ . These time constraints will be referred to as the BICON conditions. During the first step under the BICON conditions, the charge across  $C_d$  will increase approximately linearly with time, but  $C_d$  will never become fully charged. When the potential is switched to  $-E_{app}$  at  $t = \tau_p$ ,  $C_d$  will discharge the same number of coulombs accumulated during the first step, resulting in a voltage drop across the cell due exclusively to  $R_s$ . In our actual experiments,  $\tau_p$  was on the order of  $R_f C_f$ , and the response time of the

(10) Alpuche-Aviles, M. A.; Wipf, D. O. *Anal. Chem.* **2001**, *73*, 4873.

(11) Katemann, B. B.; Inchauste, C. G.; Castro, P. A.; Schulte, A.; Calvo, E. J.; Schuhmann, W. *Electrochim. Acta* **2003**, *48*, 1115.

(12) Bard, A. J.; Faulkner, L. R. *Electrochemical Methods*; Wiley: New York, 2001; p 15.

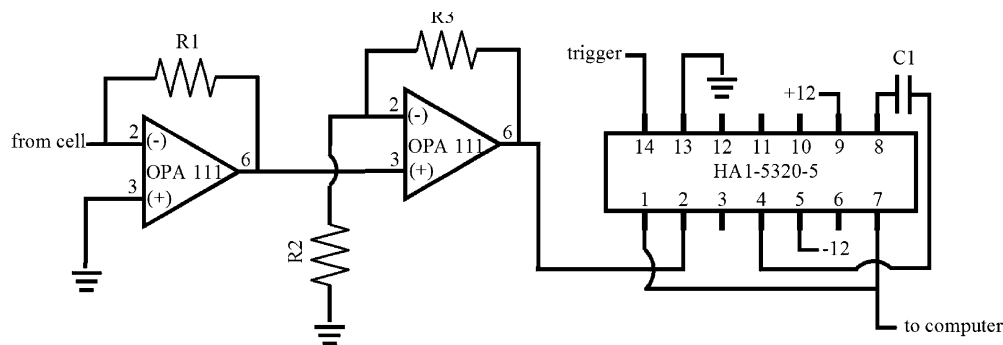


**Figure 2.** Current amplifier circuit. R1, R2, and R3 vary depending on experimental goals. Values used in this work: R1 = 1–10 M $\Omega$ , R2 = 1 k $\Omega$ , R3 = 10 k $\Omega$ , C1 = 220 pF.

amplification circuitry attenuated the output, resulting in currents that underestimated the solution conductance. Further ramifications of working outside of the BICON conditions will be discussed below.

## EXPERIMENTAL SECTION

Milli-Q 18 M $\Omega$ -cm water (Millipore, Billerica, MA) under ambient conditions was used in all procedures. Stock solutions of nominally 1 mM KCl (Mallinckrodt, Paris, KY) were prepared and diluted to the desired concentration (typically 1–100  $\mu$ M). Microelectrodes were fabricated using the procedure described previously.<sup>13</sup> Platinum wire (Goodfellow, Devon, PA) with a diameter of 125, 25, or 5  $\mu$ m was sealed in borosilicate glass, polished, and sharpened with 240 and 1200 grit paper disks (Buehler, Lake Bluff, IL). Unlike standard microelectrodes used for amperometric measurements, the conductometric tips used in this study were not polished with alumina. The residual roughness of the conductometric tips resulted in an increased double layer capacitance that is beneficial to the BICON measurements (vide infra). Before the BICON measurements, electrodes were characterized by cyclic voltammetry and amperometric SECM approach curves.

Experiments were performed with the cell in a Faraday cage. Waveform generation and data acquisition were controlled using custom LabView software and an E-series data acquisition board (AT-MIO-16E-10; National Instruments, Austin, TX) with a CB-68LP connector block. A square-wave pulse (Figure 1) with an amplitude ( $E_{\text{app}}$ ) from 10 to 500 mV and a plateau time ( $\tau_p$ ) from 10 to 250  $\mu$ s was applied between the tip and a Pt counter electrode. Two counter electrode configurations were used: either a Pt wire remote from the tip or a Pt disk sealed in glass, which also served as the substrate electrode for SECM measurements. The current was measured using a dual-stage amplifier consisting of two OPA 111 operational amplifiers followed by a sample and hold circuit (HA1-5320-5). A schematic of the circuit is given in Figure 2.

Positioning of the electrode was accomplished using an inchworm motor driven by a Burleigh 6000ULN control module and custom LabView software. Conductivity versus concentration measurements were made by successive additions of a known volume of stock solution to the cell and averaging 100 measurements with an acquisition rate ranging from 0.1 to 2 kHz.

The feedback circuit used in this work consisted of a first stage inverting amplifier with a feedback resistance ranging from 1 to 10 M $\Omega$  (R1 in Figure 2). The second stage was a noninverting amplifier with an 11-times gain (R2 = 1 k $\Omega$ , R3 = 10 k $\Omega$ ). The noninverting second stage also behaves as a buffer between the first stage and the operational amplifiers of the sample and hold. The total feedback resistance,  $R_f$ , as well as the stray capacitance in the feedback loop,  $C_f$ , were measured by replacing the cell with a known resistance. By measuring the output as a function of  $E_{\text{app}}$ , one obtains the ratio of  $R_f$  to  $R_s$  from the slope. The feedback capacitance was obtained by fitting the output as a function of  $\tau_p$  curve to an exponential function with a time constant of  $R_f C_f$ .

## RESULTS AND DISCUSSION

**Conductivity Measurements.** The application of the BICON method to very small electrodes requires consideration of the effects caused by the very small capacitances of the electrodes and the small currents (typically picoamperes to nanoamperes) that result from the potential steps. Microelectrodes with diameters of 125, 25, and 5  $\mu$ m were used in this study. While the 125- $\mu$ m-diameter electrode is larger than what is typically used in SECM techniques, the increased size allowed for proof of concept experiments owing to its relatively low effective cell constant (vide infra). The conductance versus concentration curve obtained for KCl solutions at a 125- $\mu$ m-diameter Pt electrode with  $E_{\text{app}} = 25$  mV,  $\tau_p = 100$   $\mu$ s, and  $R_f = 102$  M $\Omega$  is shown in Figure 3. A linear relationship between conductance and concentration is expected, assuming a constant molar conductivity over the concentration range of interest. This assumption is valid for KCl solutions up to 1 mM<sup>14</sup> within a 2% error.

To analyze the data using eq 4,  $R_s$  and  $C_d$  must be expressed as functions of concentration,  $c$ . The solution resistance is related to electrolyte concentration through the molar conductivity,  $\Lambda^\circ$ , of the salt,

$$R_s = \frac{k_{\text{cell}} (\text{cm}^{-1})}{\Lambda (\Omega^{-1} \text{cm}^2 \text{mol}^{-1}) c (\text{mol cm}^{-3})} \quad (6)$$

where  $k_{\text{cell}}$  is the conductivity cell constant. For a typical conductivity cell consisting of two equal-area, closely spaced, parallel plates, the cell constant is the distance between the electrodes

(13) Fan, F. F.; Demaille, C. In *Scanning Electrochemical Microscopy*; Bard, A. J., Mirkin, M. V., Eds.; Marcel Dekker: New York, 2001.

(14) Lind, J. E., Jr.; Zwolenik, J. J.; Fuoss, R. M. *J. Am. Chem. Soc.* **1959**, *81*, 1557.

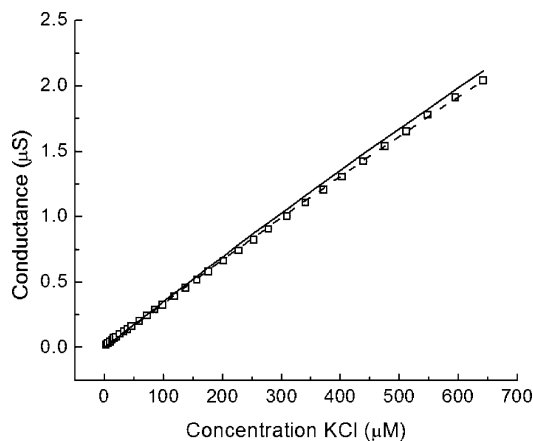


**Figure 3.** Conductance versus concentration plot obtained with a 125- $\mu\text{m}$ -diameter electrode.  $E_{\text{app}} = 25$  mV,  $\tau_p = 100$   $\mu\text{s}$ ,  $R_f = 102$  M $\Omega$ . Legend: squares, experimental data; solid line, theory using eq 4; dashed line, theory with increasing  $C_f$  from 0.31 to 0.39 pF (see text).

divided by the electrode area. Newman<sup>15</sup> has shown that the effective cell constant for a microdisk in an insulating plane remote from a large counter electrode is  $1/4r$ , where  $r$  is the electrode radius. For a 125  $\mu\text{m}$  diameter electrode, this results in a cell constant of 40  $\text{cm}^{-1}$ . At low concentrations, the double layer capacitance can be approximated from Guoy–Chapman theory,

$$C_d (\mu\text{F}) \cong \pi r^2 230 \sqrt{c (\text{mol L}^{-1})} \quad (7)$$

where  $r$  is the radius of the tip in centimeters. Using 149.93  $\Omega^{-1} \text{mol cm}^{-2}$  for the limiting molar conductivity of KCl,<sup>14</sup> one obtains reasonable agreement between theory and experiment. Note that substituting eqs 6 and 7 into eq 4 results in a fit that contains no adjustable parameters. The capacitance of the feedback loop,  $C_f$ , was estimated, using the procedure described in the Experimental Section, to be 0.31 pF. An increase in  $C_f$  to 0.39 pF results in a very good fit of the data obtained at a 125- $\mu\text{m}$ -diameter electrode (Figure 3, dashed line). The source of this capacitance is not clear; it is not associated with the capacitance of the first amplification stage. Two circuit configurations differing in the size of the first stage resistor and second stage gain but resulting in the same amplification produced the same value of  $C_f$ .<sup>16</sup>

Results deviated from the theoretically expected response for smaller electrodes. Figure 4 shows a similar plot of conductance versus KCl concentration for BICON pulses ( $\tau_p = 20$   $\mu\text{s}$ ) applied to a 5- $\mu\text{m}$ -diameter Pt tip. As with the larger electrode, the plots are linear up to KCl concentrations of 1 mM. Unlike the larger electrode, a linear response is not expected if eqs 6 and 7 are used to calculate the solution resistance and double layer capacitance, respectively (solid line in Figure 4). One finds that Guoy–Chapman theory underestimates  $C_d$ . An increase in the double layer capacitance to 130  $\mu\text{F}/\text{cm}^2$  is needed to obtain a good fit (dashed line in Figure 4). Although it is likely that the true double layer capacitance of the 5- $\mu\text{m}$  tip used in this experiment is larger than predicted by Guoy–Chapman theory, the value

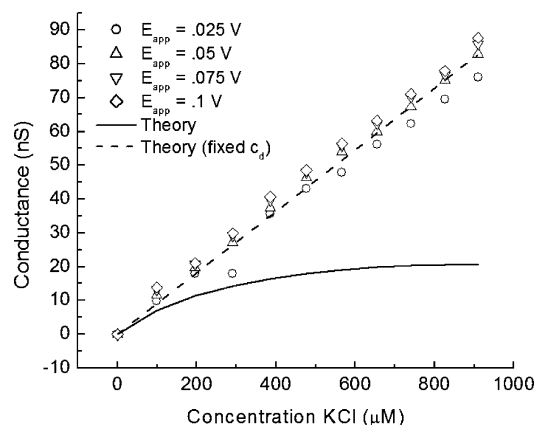


**Figure 4.** Conductance versus concentration plots obtained using a 5- $\mu\text{m}$ -diameter electrode.  $E_{\text{app}} =$  see legend,  $\tau_p = 20$   $\mu\text{s}$ ,  $R_f = 102$  M $\Omega$ . Dashed line is theory calculated using Guoy–Chapman double layer capacitance; solid line is theory using  $C_d$  as a concentration-independent adjustable parameter.

needed is too large, even when one takes surface roughness into account, so that  $C_d$  in this case should be considered as an adjustable parameter. The double layer capacitance of a solid polycrystalline Pt disk is extremely sensitive to solution impurities, specific adsorption of solutes, and the presence of an oxide film on the surface.<sup>17</sup> Unless noted otherwise, we will use 40  $\mu\text{F}/\text{cm}^2$  as an approximation for the Pt double layer capacitance under our conditions and assume no concentration dependence. A final point about the data in Figure 4 is that different values of  $E_{\text{app}}$  result in the same conductance. This is expected, considering the solution contains no electroactive species within the potential range used in the BICON pulses. The discrepancies observed when small (25 mV) values are used for  $E_{\text{app}}$  are probably caused either by errors in measuring the correspondingly small currents under these conditions or by lack of accurate subtraction of the background current. The sensitivity of a BICON measurement is proportional to  $E_{\text{app}}$  so long as the rise time of the waveform generator is sufficiently fast and no faradaic processes occur within the applied potential range.

Since the solution conductance depends linearly on the electrode radius through the cell constant, one would expect a difference by a factor of 25 when comparing conductances measured with the 125- and 5- $\mu\text{m}$  diameter electrodes. From Figures 3 and 4, the conductance of 600  $\mu\text{M}$  KCl at the 125- $\mu\text{m}$  electrode ( $E_{\text{app}} = 25$  mV,  $\tau_p = 100$   $\mu\text{s}$ ) is 1.9  $\mu\text{S}$ , and the comparable value at the 5- $\mu\text{m}$  electrode ( $E_{\text{app}} = 25$ –100 mV,  $\tau_p = 20$   $\mu\text{s}$ ) is 56 nS. The difference between the two numbers, a factor of 35, cannot be accounted for by electrode geometry considerations alone. Furthermore, the theoretical solution conductance for the two electrodes, calculated using the inverse of eq 6, are 2.2  $\mu\text{S}$  and 90 nS for the 125- and 5- $\mu\text{m}$  electrodes, respectively. The reason for these discrepancies lies in the sensitivity of the measurements for the smaller electrode to the BICON conditions, for example, the value selected for  $\tau_p$ .

To analyze the conductance discrepancies further, it is useful to determine the BICON conditions. On the basis of measurements made with resistors, the resistance and capacitance of the

(15) Newman, J. J. *Electrochem. Soc.* **1966**, *113*, 501.

(16) The slew rate of the operational amplifiers could also contribute to  $C_f$ ; however, the OPA-111 has an average slew rate of 2 V/ $\mu\text{s}$ .

(17) Pell, W. G.; Zolfaghari, A.; Conway, B. E. *J. Electroanal. Chem.* **2002**, *532*, 13.

feedback loop can be estimated, resulting in a feedback time constant of  $\sim 30 \mu\text{s}$  for our system with a  $102 \text{ M}\Omega$  feedback loop. The solution time constant,  $R_s C_d$ , is dependent on the electrode size and scales with  $r$ . Using  $40 \mu\text{F}/\text{cm}^2$  for the double layer capacitance of a Pt microelectrode, one finds solution time constants of  $2.2 \text{ ms}$  and  $87 \mu\text{s}$  for the  $125\text{-}\mu\text{m}$  and  $5\text{-}\mu\text{m}$  electrodes, respectively. The BICON conditions require that  $\tau_p$  be larger than the feedback time constant and smaller than the solution time constant. The choice of  $\tau_p$  satisfies the upper limit of the BICON conditions in both cases, although for the  $5\text{-}\mu\text{m}$  electrode, a  $r_{\text{solution}}$  of  $\sim 0.23$  is slightly larger than desirable. The  $\tau_p$  selected for the  $125\text{-}\mu\text{m}$  electrode,  $100 \mu\text{s}$ , is  $\sim 4$  times longer than the feedback time constant, but the plateau time used for the  $5\text{-}\mu\text{m}$  electrode,  $20 \mu\text{s}$ , is too small, given the slow response time of the current amplifier, so that the current measured at the  $5\text{-}\mu\text{m}$  electrode will underestimate the solution conductance. Substituting into eq 5 the appropriate values for  $r_{\text{feedback}}$  and  $r_{\text{solution}}$ , one finds the theoretical current should underestimate the solution conductance by 4% at the  $125\text{-}\mu\text{m}$  electrode and 55% for the  $5\text{-}\mu\text{m}$  electrode. The actual currents underestimate the conductance by 15% at the  $125\text{-}\mu\text{m}$  electrode and 39% at the  $5\text{-}\mu\text{m}$  electrode. When working outside of the BICON conditions, the agreement between theory and experiment will depend very strongly on the accurate measurement of  $C_f$  and  $C_d$ . Despite the inability to convert the observed current into a solution conductance under these conditions, a linear relationship is observed between the electrolyte concentration and the BICON output, demonstrating that calibration curves can facilitate quantification of data when  $C_f$  and  $C_d$  cannot be determined.

Johnson and Enke developed the BICON technique for use with large electrodes. When the technique is applied to microelectrodes, the lower limit to the selection of a plateau time is no longer the time constant arising from stray capacitance and the output impedance of the data acquisition board (a value expected to be negligible on the microsecond time scale), but rather, the large amount of amplification required to make a conductance measurement at a microelectrode. From eq 5, an error of  $\sim 3\%$  in the conductance is observed when  $\tau_p$  is 4 times the feedback time constant and  $1/10$  the solution time constant. If we desire such accuracy for the measurement of a  $600 \mu\text{M}$  solution at a  $5\text{-}\mu\text{m}$  tip, a step time no larger than  $9 \mu\text{s}$  must be used. Thus, the feedback time constant should be  $< 2 \mu\text{s}$ . Assuming  $0.3 \text{ pF}$  for the value of  $C_f$ , the feedback loop must contain a resistance of  $7 \text{ M}\Omega$  or less.

The following data demonstrate the importance of selecting an appropriate plateau time when measuring solution conductance using a microelectrode with a small  $C_d$ . Figure 5 shows conductance versus concentration plots at various values of  $\tau_p$  obtained with a  $5\text{-}\mu\text{m}$ -diameter electrode with a lower  $C_d$  ( $\sim 10 \mu\text{F}/\text{cm}^2$ ) than the one used above. The feedback loop was reduced to  $21.6 \text{ M}\Omega$  to minimize  $R_f C_f$  without compromising sensitivity. At step times longer than  $10 \mu\text{s}$ , the plot is severely distorted by double layer capacitance and little, if any, information regarding the solution conductance can be extracted. At  $\tau_p = 10 \mu\text{s}$ , the conductance versus concentration plot is linear, with a slope that is  $\sim 60\%$  that of the theoretical slope. The lower limit,  $R_f C_f$ , is independent of solution properties, whereas the upper limit,  $R_s C_d$ , is not. If the upper limit of the BICON conditions is always

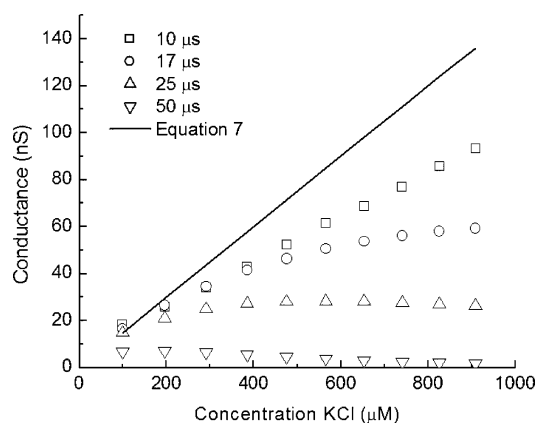


**Figure 5.** Conductance versus concentration plots obtained using a  $5\text{-}\mu\text{m}$ -diameter electrode with various plateau times (see legend).  $E_{\text{app}} = 200 \text{ mV}$ ,  $R_f = 21.6 \text{ M}\Omega$ . Solid line is the conductance of the solution expected based on eq 7.

adhered to, then the current from a BICON pulse will be proportional to the electrolyte concentration. Under these conditions, the BICON technique can still provide the solution conductance through the use of a calibration curve.

The usefulness of the BICON technique applied to microelectrodes depends strongly on experimental conditions that allow for a plateau time that lies within the BICON criteria. Since the solution conductance is proportional to  $r^{-1}$  and the solution time constant is proportional to  $r$ , the move to smaller electrodes necessitates a shorter  $\tau_p$  and greater sensitivity (i.e., a larger  $R_f$ ). Greater sensitivity comes at the expense of a lower limit for the BICON conditions that might be longer than the desired plateau time. The implication of working below the BICON conditions is a response that is not amplified as much as desired. On the other hand, exceeding the upper limit of the BICON conditions results in a response that contains a capacitive component that may be unknown but must be included in the analysis. Ultimately, the BICON technique will be limited by the length of the shortest pulse that can be supplied by the waveform generator and the precision at which the detection system can measure millivolt changes. For this technique to be a viable method for measuring conductance at a microelectrode, it is necessary to use the shortest  $\tau_p$  possible such that  $C_d$  does not interfere with the linearity of the conductance-vs-concentration plot and introduce uncertainty into the measurement.

Ideally, one would like to extend conductance measurements at a microelectrode to electrolyte concentrations on the order of  $0.1 \text{ M}$ . At a  $25\text{-}\mu\text{m}$ -diameter electrode,  $0.1 \text{ M KCl}$  would result in a  $R_s$  of  $13 \text{ k}\Omega$  and a solution time constant of  $\sim 2 \mu\text{s}$ . To achieve a theoretical error better than  $10\%$  would require a  $\tau_p$  of  $< 1 \mu\text{s}$  with  $R_f = 500 \text{ k}\Omega$ . Under these conditions and an  $E_{\text{app}}$  of  $25 \text{ mV}$ , a  $10\%$  change in the solution conductance will give rise to an appreciable  $30\text{-mV}$  change in the output. For a  $1\text{-}\mu\text{m}$ -diameter electrode, the solution resistance and time constant for  $0.1 \text{ M KCl}$  are  $333 \text{ k}\Omega$  and  $100 \text{ ns}$ , respectively. Measurements made under these conditions would require essentially no stray capacitance in the feedback loop such that  $C_f$  is limited by the choice of operational amplifiers used.

**SECM Approach Curves.** The measurement of solution conductance as a tip is brought close to an insulating substrate has been previously shown to follow the same theory as the

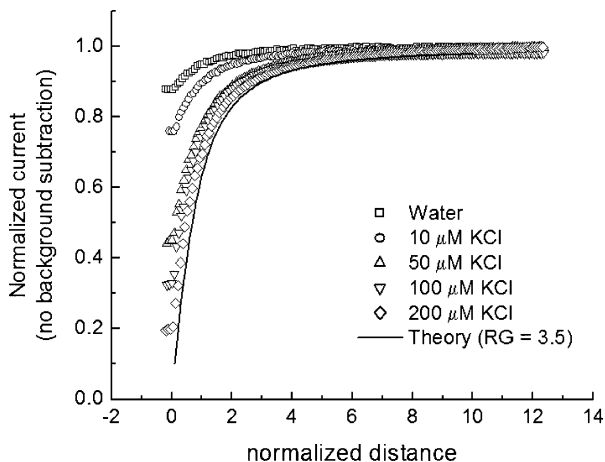


**Figure 6.** Approach of a 25- $\mu\text{m}$ -diameter Pt tip to an insulating substrate in KCl solutions of varying concentration. The distance axis is normalized by the tip radius, and the conductance axis is normalized by the conductance measured with the tip remote from the surface.  $E_{\text{app}} = 400 \text{ mV}$ ,  $\tau_p = 33 \mu\text{s}$ , approach rate =  $1 \mu\text{m/s}$ .

analogous amperometric technique.<sup>9</sup> Figure 6 shows the conductance measured at a 25- $\mu\text{m}$ -diameter Pt tip as a function of normalized distance,  $L$  (where  $L = d/r$ , and  $d$  is the distance between tip and substrate) as it approaches an insulating substrate with different KCl concentrations, compared to a theoretical curve for the amperometric (negative feedback) response.<sup>9,13</sup> As shown, the experimental curves lie above the theoretical one, and the raw approach curves (not shown) obtained in this study appear to approach a nonzero conductance at  $L = 0$  that is independent of electrolyte concentration. Wipf et al.<sup>18</sup> have observed capacitive coupling between the shaft of microelectrodes and the counter electrode. This residual conductivity in BICON/SECM at  $L = 0$  is probably due to the same effect. Qualitatively, one would expect the background current to increase as more of the electrode is immersed into the solution and can contribute to the coupling. Such a current increase was observed, but the magnitude of the increase was too small to account for all of the deviation in the approach curves. Residual current can be corrected for when approach curves are obtained at multiple electrolyte concentrations. The current at which the electrode touches the surface, as evidenced by a sharp deviation in the approach curve, was found to be similar for each electrolyte concentration. The approach curves were fit to theory by subtracting this current so that each electrolyte concentration gave the same approach curve (Figure 7). This approach to background subtraction assumes that the background current is concentration-independent. The validity of this assumption may contribute to the slight discrepancies observed at normalized distances below 0.25. BICON/SECM (and presumably conductivity techniques in general) can be used to perform an approach curve in a solution with no intentionally added electrolyte (note the line for pure water line in Figure 7).

The nature of BICON approach curves with a conducting substrate depends on electrolyte concentration. Figure 8 shows the dependence of the feedback response on the electrolyte concentration as a 25- $\mu\text{m}$  tip is brought close to a 3-mm-diameter Pt disk at open circuit potential (OCP). For a BICON pulse with

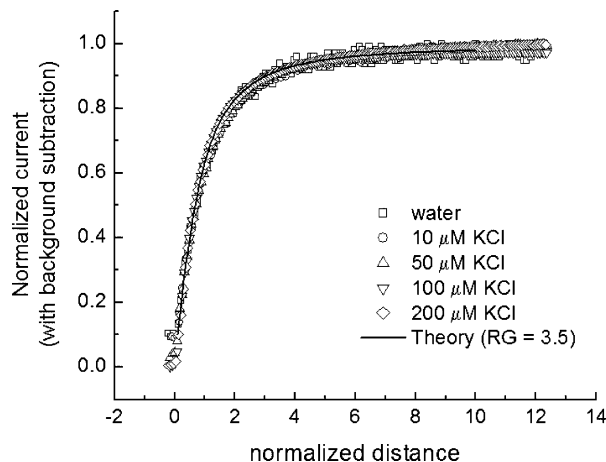


**Figure 7.** Approach curves as in Figure 6 with the background conductance subtracted from the measured conductance. The amount of background conductance was adjusted such that a single value would result in concentration-independent approach curves.

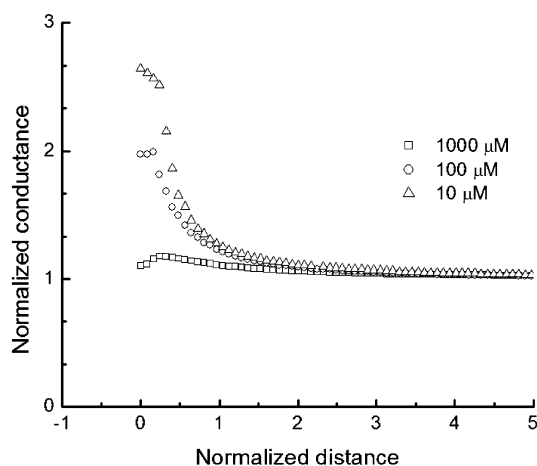


**Figure 8.** Approach of a 25- $\mu\text{m}$ -diameter Pt tip to a 3-mm Pt substrate at open circuit potential in KCl solutions of varying concentration. The distance and conductance are normalized as in Figure 6. The distance normalization is approximate.  $E_{\text{app}} = 100 \text{ mV}$ ,  $\tau_p = 20 \mu\text{s}$ , approach rate =  $1 \mu\text{m/s}$ .

$E_{\text{app}} = 100 \text{ mV}$  and  $\tau_p = 20 \mu\text{s}$ , positive feedback was observed when the concentration of KCl ranged from  $10 \mu\text{M}$  to  $1 \text{ mM}$ . The amount of positive feedback, normalized to the conductance remote from the surface, decreased with increasing electrolyte concentration. Analogous behavior was observed if the substrate, rather than a remote Pt counter electrode, was used. As expected, the measured conductance was independent of  $E_{\text{app}}$ .

The shape of approach curves also depended on  $\tau_p$ . Figure 9 shows the normalized approach of a 25- $\mu\text{m}$  tip to a 3-mm-diameter Pt disk in  $1 \text{ mM}$  KCl for  $\tau_p$  values of 21–67  $\mu\text{s}$  ( $E_{\text{app}} = 100 \text{ mV}$ , approach rate =  $1 \mu\text{m/s}$ ). At small  $\tau_p$ , positive feedback was observed. The amount of feedback diminished and turned into a negative feedback response for  $\tau_p > 33 \mu\text{s}$ . Figure 10 shows the relationship between the measured conductance and  $\tau_p$  for the electrode  $\sim 5$  and  $100 \mu\text{m}$  from the substrate surface. The data clearly show that at short plateau times, the measured conductance close to the surface is higher than when the electrode is moved away from the surface. The magnitude of the difference decreases and eventually inverts as  $\tau_p$  is increased. Table 1 lists the values of  $R_s$  and  $C_d$  necessary to fit the shape of the measured

(18) Wipf, D. O.; Michael, A. C.; Wightman, R. M. *J. Electroanal. Chem. Interfacial Electrochem.* **1989**, *269* (1), 15.

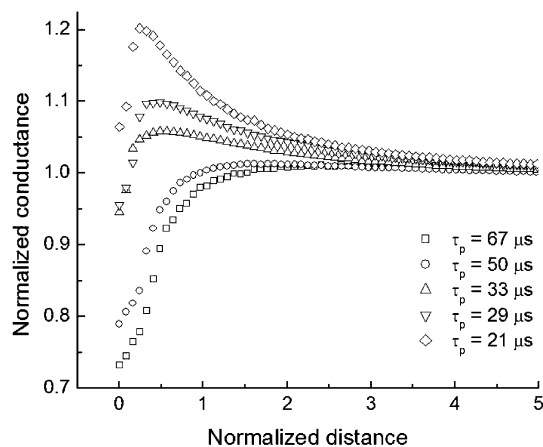


**Figure 9.** Approach of a 25- $\mu\text{m}$ -diameter Pt tip to a 3-mm Pt substrate at open circuit potential in 1 mM KCl with varying plateau times as indicated in the legend. The distance and conductance are normalized as in Figure 6. The distance normalization is approximate.

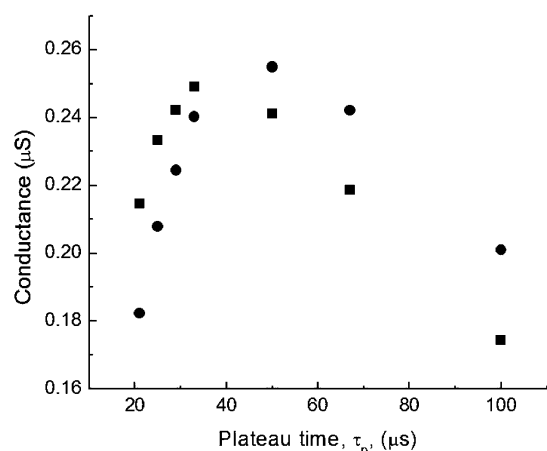


**Figure 10.** Measured conductance as a function of plateau time,  $\tau_p$ , at a 25- $\mu\text{m}$ -diameter Pt tip 5 (squares) or 100  $\mu\text{m}$  (circles) from a conductive substrate at open circuit potential.

**Table 1.  $R_s$  and  $C_d$  Used to Fit Several Points along the Approach Curves Shown in Figure 9**

L	$C_d$ (pF)	$R_s$ (M $\Omega$ )	$R_s C_d$ ( $\mu\text{s}$ )
6	30	2.9	87
2	30	2.8	84
1.44	30	2.75	82
0.96	27	2.6	70
0.72	25	2.5	62
0.48	23	2.39	55
0.25	20	2.25	45

conductance versus  $\tau_p$  plot for several points along the approach curves in Figure 9. As the distance between tip and substrate decreases, both  $R_s$  and  $C_d$  decrease. A decrease in the measured solution resistance in the vicinity of a conducting substrate has been observed previously in SECM<sup>9</sup> and other techniques employing AC resistance measurements.<sup>19,20</sup> This is caused by a redirection of the current distribution through the conductor, which has a significantly lower resistance than the surrounding solution. The

(19) Leroy, C.; Fransaer, J.; Celis, J. P. *Proc. Electrochem. Soc.* **1998**, 98–10, 186.

(20) Perez, A. T. *J. Electrostat.* **2002**, 56, 199.

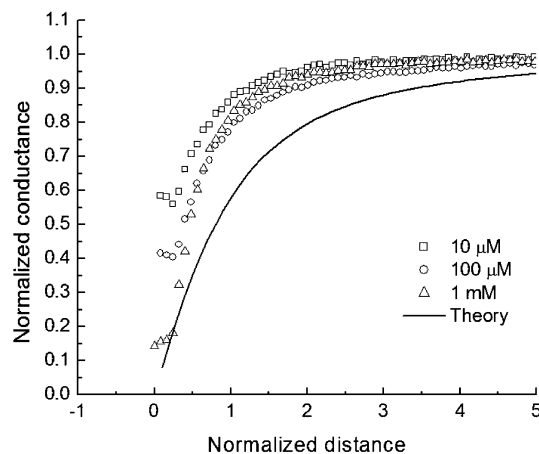


**Figure 11.** Approach of a 25- $\mu\text{m}$ -diameter Pt tip to a 127- $\mu\text{m}$  Pt substrate at open circuit potential in KCl solutions of varying concentration. The distance and conductance are normalized as in Figure 6. The distance normalization is approximate.  $E_{\text{app}} = 100$  mV,  $\tau_p = 20$   $\mu\text{s}$ , approach rate = 1  $\mu\text{m/s}$ .

exact nature of the decrease of  $C_d$  is less clear, but probably involves coupling of the tip to the substrate.

The size of the conductive substrate will influence the magnitude of the positive feedback, since smaller substrates will provide less redirection of the current distribution. Figure 11 shows the approach curves of a 25- $\mu\text{m}$  Pt tip to a 127- $\mu\text{m}$  Pt substrate for several electrolyte concentrations. In each case, negative feedback is observed; however, the approach curve lies above the theoretical curve for purely negative feedback. Both redirection of the current distribution due to the conductive substrate as well as the presence of residual background conductivity can account for the observed increase in current. When the 127- $\mu\text{m}$  substrate is used as the counter electrode, slight positive feedback is observed at low concentrations of electrolyte. A quantitative rationalization of this behavior will require calculation of changes in  $C_d$  and  $R_s$  as the tip approaches the substrate.

A decrease in  $C_d$  and  $R_s$  naturally leads to a decrease in the solution time constant. For the data shown in Figure 9, the solution time constant is 87  $\mu\text{s}$  at large tip-substrate distances and decreases to 45  $\mu\text{s}$  as the tip approaches the surface (Table 1). At  $\tau_p = 50$  and 67  $\mu\text{s}$ , the data with the tip close to the surface are acquired with a plateau time outside of the BICON conditions. The shape of the approach curve is, thus, highly dependent on the data acquisition parameters. The same analysis can be made of the concentration dependence observed in Figure 8. At low electrolyte concentrations, the solution time constant is larger. Even though it decreases with decreasing tip-substrate distance, the upper limit of the BICON conditions does not cross below the plateau time. Increasing the electrolyte concentration decreases the solution time constant, bringing the upper limit of the BICON conditions close to  $\tau_p$ .

Figure 12 summarizes the time constant behavior, calculated using eqs 6 and 7, of an electrolyte solution as a function of electrolyte concentration and electrode size. The shortest  $\tau_p$  for our instrumentation is 10  $\mu\text{s}$ ; thus, the shortest time constant that can be reliably measured with this instrumentation is 100  $\mu\text{s}$ . With a 125- $\mu\text{m}$ -diameter electrode, KCl solutions up to 0.1 M can be investigated without approaching the BICON upper limit. It is clear, however, that micrometer-sized electrodes will require

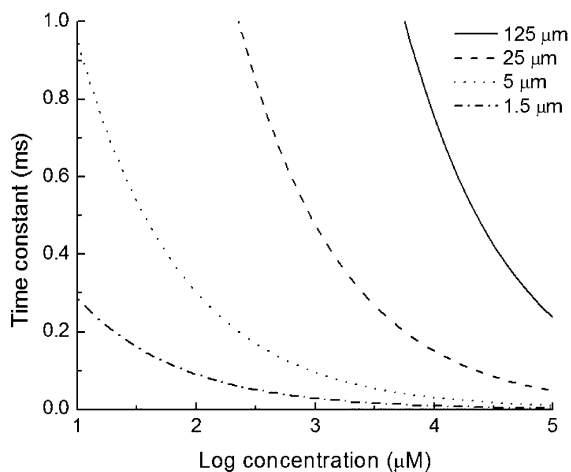


**Figure 12.** Estimated time constants, calculated using eqs 6 and 7, for KCl solutions measured at electrodes from 125 to 1.5  $\mu\text{m}$  in diameter.

values for  $\tau_p$  in the submicrosecond range in order to measure the conductance of concentrated solutions.

## CONCLUSION

The bipolar conductance (BICON) method of measuring solution conductance has been applied to ultramicroelectrodes and as a conductometric mode for SECM. Under these conditions, the lower limit of the plateau time,  $\tau_p$ , is governed by the finite response time of the amplification circuit and the upper limit, as described in the original work by Johnson and Enke,<sup>1</sup> is governed by the double layer capacitance of the electrode and the solution resistance. Decreasing the ultramicroelectrode size reduces the range of plateau times that lie within the BICON conditions, making direct measurement of solution conductance from the electrode current difficult. Nevertheless, as long as the upper limit of the BICON conditions is met, the current from a BICON pulse is proportional to electrolyte concentration at electrodes with diameters as small as 5  $\mu\text{m}$  so that solution conductance can be obtained through the use of calibration curves. The use of BICON to measure solution conductance at ultramicroelectrodes is limited by two factors: the applied pulse widths and the rise time of the amplification circuitry. For example, the measurement of 0.1 M solutions with 1- $\mu\text{m}$ -diameter electrodes will require instrumentation capable of generating 100-ns pulse sequences and amplification circuits with appropriately fast rise times.

BICON approach curves were performed over insulating and conductive substrates. For insulating substrates, the approach curves displayed negative feedback behavior. When residual current, likely due to capacitive coupling of the ultramicroelectrode, was corrected for, the approach curves fit amperometric negative feedback theory. Such a background correction can be accomplished by measuring approach curves in solutions with different electrolyte concentrations and noting the similar current at which the electrode touches the substrate. With BICON/SECM

and presumably with other AC techniques, it is possible to obtain approach curves in solutions with no intentionally added electrolyte. Over a large conductive substrate, positive feedback was observed; however, the behavior did not agree with amperometric positive feedback theory. Analysis of the solution resistance and double layer capacitance as a function of tip/substrate distance showed that the limits of the BICON conditions shifted as the electrode approached the surface. Changes in the solution time constant led to a decrease in the BICON current, since the upper limit of the BICON conditions became less than the plateau time used to obtain the approach curve. Careful selection of the plateau time is required to ensure it remains within the BICON conditions throughout the approach curve. Since positive feedback over a conductive substrate is due to changes in the current distribution, the substrate size will influence the nature of BICON/SECM feedback. This has been observed when comparing the approach of a 25- $\mu\text{m}$  Pt ultramicroelectrode to 3-mm and 127- $\mu\text{m}$  diameter Pt substrates.

## DEFINITIONS

$c$	concentration (mol mL <sup>-1</sup> or M)
$C_d$	electrode double layer capacitance ( $\mu\text{F}$ )
$C_f$	stray capacitance in the amplifier circuit ( $\mu\text{F}$ )
$C_p$	stray capacitance in the electrode leads ( $\mu\text{F}$ )
$E_{\text{app}}$	applied potential (mV)
$i$	current (A)
$k_{\text{cell}}$	conductivity cell constant (cm <sup>-1</sup> )
$L$	tip/substrate distance normalized by the tip radius
$\Lambda^\circ$	limiting molar conductivity ( $\Omega^{-1} \text{cm}^2 \text{mol}^{-1}$ )
$Q$	charge (C)
$r$	tip radius (cm)
$r_{\text{feedback}}$	ratio of plateau time to the feedback time constant ( $\tau_p / R_f C_f$ )
$r_{\text{solution}}$	ratio of plateau time to the solution time constant ( $\tau_p / R_s C_d$ )
$R_f$	total feedback resistance of the signal amplifier ( $\Omega$ )
$R_s$	solution resistance ( $\Omega$ )
$t$	time ( $\mu\text{s}$ )
$\tau_p$	plateau time ( $\mu\text{s}$ )
$V_{C_d}$	voltage drop across double layer capacitance (V)
$V_{R_s}$	voltage drop across solution (V)

## ACKNOWLEDGMENT

We thank International SEMATECH for financial support of this work.

Received for review August 2, 2004. Accepted September 15, 2004.

AC048867T